In Silico Evaluation of Local Hemodynamics Following Vena Cava Filter Deployment

J. Ferdous[1], M. Ghaly[2], Fatematuzzahan[1], and T. Shazly[*1,3]
[1]Biomedical Engineering Program, University of South Carolina, SC, [2]Department of Biomedical Engineering, North Carolina State University, NC, [3]Department of Mechanical Engineering, University of South Carolina, SC
*Corresponding author: 300 Main Street, Columbia, SC-29208. Email: shazly@cec.sc.edu

Abstract:

Inferior vena cava (IVC) filters have become essential components in deep vein thrombosis treatment, and are particularly critical for preventing pulmonary embolisms in anticoagulation-resistant patients. Filter efficacy relies on maintaining IVC patency, or openness, by preventing filter-induced thrombosis following clot capture. A computational fluid dynamics (CFD) model has been developed to determine whether a candidate filter design elicits hemodynamic patterns that promote thrombus development. The CFD model yielded a steady-state flow solution describing blood velocity in the vicinity of an impermeable filter with various levels of clot accumulation. Filter and clot geometries were created based on filter explants after clot capture. Porous media flow within the clot was characterized using the Brinkman equations, whereas Non-Newtonian blood flow within the IVC was modeled using the Navier-Stokes equations. Clot porosity and permeability values were varied to simulate clot accumulation over time. Decreasing clot porosity and permeability resulted in higher wall shear stress (WSS), suggesting that clot maturity modulates thrombotic potential. Filter edge velocity increased from unoccluded to occluded filter state with nonuniform longitudinal and radial shear stress patterns, indicating that local thrombogenicity varies with both clot state and position.

Keywords: Vena cava filter, Hemodynamics, Thrombogenicity, Wall shear stress, Occlusion.

1. Introduction

Deep vein thrombosis (DVT), development of blood clot in the deep vein of the lower extremity, is a common clinical problem. Transport of detached blood clot through the bloodstream to an artery in the lungs can restrict downstream blood supply and results pulmonary embolism (PE), a potentially life-threatening complication. Venous thromboembolism (VTE), defined as DVT, PE, or both, affects an estimated 300,000-600,000 individuals in the United States each year, causing considerable morbidity and mortality [1].

Inferior vena cava (IVC) filter have been widely used for the patients with high risk for DVT, and who are unresponsive to or who have contraindications to anticoagulation therapy. Though several filters are available in the market for clinical usage and can reduce the risk of PE, they introduce a new set of considerations to clinical safety and efficacy. Foremost among these issues is the increase in late recurrent DVT at the implantation site [2]. Vascular injury during filter implantation and/or change in local hemodynamics either due to the filter design or trapped blood clot could cause DVT [3].

Local hemodynamics adjacent to the filter plays an important role in determining filter efficiency. Low wall shear stress (WSS) regions and recirculation zones favor thrombin and fibrin accumulations hence, promote thrombosis. On the other hand, high WSS regions can activate platelets aggregation and results primary hemostasis. However, High WSS regions can also enhance the removal of thrombin and fibrin and reduces the possibility of secondary hemostasis [4]. A computational fluid dynamics (CFD) based model offers an efficient and complementary framework for critical implant assessment and facilitates both understanding and prediction of local hemodynamics following IVC filter deployment.

We present a three-dimensional (3D) computational model to evaluate the performance of a candidate IVC filter. The changes in velocity profiles and WSS due to accumulation of clot over time are computed. The results provide valuable insights on the
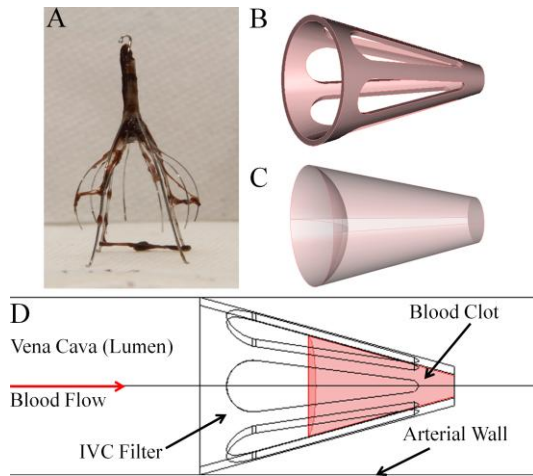
Figure 1. Clinical image of clot capture (A), inferior vena cava geometry (B), Clot geometry as conical shape with elliptical void (C), and schematic of the two-dimensional computational domain (not to scale) (D).

interplay between filter design and the potential for filter-induced DVT.

2. Methods

A three-dimensional computational model was constructed with geometrical regions representing an IVC filter, blood clot, and inferior vena cava (lumen) (Figure 1). Computer-aided design was used to develop the candidate IVC filter, whereas blood clot geometry having conical shape with elliptical void was developed based on the clinical images of clot capture. Filter was assumed to be deployed symmetrically in the vena cava. The diameter and length of the vena cava were 0.023 m and 0.4 m, respectively.

Blood flow through the lumen was assumed to be steady, laminar, and fully-developed, and was modeled using Navier-Stokes and continuity equations as follows:

$$\rho_L(\mathbf{u_L}.\nabla\mathbf{u_L}) = -\nabla P_L + \mu_L\nabla^2\mathbf{u_L}$$
$$\nabla.\mathbf{u_L} = 0$$

where $\mathbf{u_L}$, $\rho_L = 1060\ \mathrm{kg\ m^3}$, μ_L, and P_L are respectively luminal blood velocity, density, viscosity, and pressure. Blood was assumed as an incompressible fluid. Due to generation of low-shear rates in the regions adjacent to the implanted IVC filter and to capture shear-thinning behavior of blood, a non-Newtonian

Carreau model was used to account dynamic blood viscosity as flows:

$$\mu = \mu_\infty + (\mu_0 - \mu_\infty)[1 + (\lambda\dot\gamma)^2]^{\frac{n-1}{2}}$$

where μ is the effective blood viscosity, $\mu_\infty = 0.035\ \mathrm{g\ cm^{-1}\ s}$ and $\mu_0 = 2.5\ \mathrm{g\ cm^{-1}\ s}$ are the blood viscosities at infinite and zero shear rates, respectively, $\lambda = 25\ \mathrm{s}$ is a time constant, $n = 0.25$ is a power law index, and $\dot\gamma$ is the shear rate.

Steady blood flow through the porous clot was modeled using Brinkman and continuity equations as follow:

$$\rho_C(\mathbf{u_C}.\nabla\mathbf{u_C}) = -\nabla P_C + \left(\frac{1}{\varepsilon_C}\right)\mu_C\nabla^2\mathbf{u_C} - \left(\frac{\mu_C}{\kappa_C}\right)\mathbf{u_C}$$
$$\nabla.\mathbf{u_C} = 0$$

where $\mathbf{u_C}$, $\rho_C = 1025\ \mathrm{kg\ m^{-3}}$, $\mu_C = 4.2 \times 10^{-4}\ \mathrm{Pa-s}$, and P_C are respectively blood velocity, density, viscosity, pressure, whereas, κ_C and ε_C are respectively Darcy's permeability and porosity of the clot. To simulate the transient clot accumulation process from the early to mature stage, permeability and porosity of the clot were altered.

A steady, Poiseuille parabolic velocity profile having maximum velocity of $0.129\ \mathrm{m\ s^{-1}}$ was imposed at the luminal inlet and a zero pressure boundary condition was applied at the luminal outlet to simulate the blood flow. No-slip boundary condition was used at the mural interface and IVC filter surface. Continuity of momentum was assumed for the blood transport though the clot at blood-clot interface. However, no-slip condition was used at blood-clot interface at the mature condition, assuming the clot behaved as an impermeable solid. COMSOL Multiphysics™ was used to perform numerical simulations and the iterations were continued until the relative error tolerance magnitude reached 10^{-5}. The computational solution was considered mesh-independent when the relative change in peak WSS was less than 3% at any simulated time step between successive mesh iterations.

3. Results and Discussion

3.1: Effect of non-Newtonian viscosity

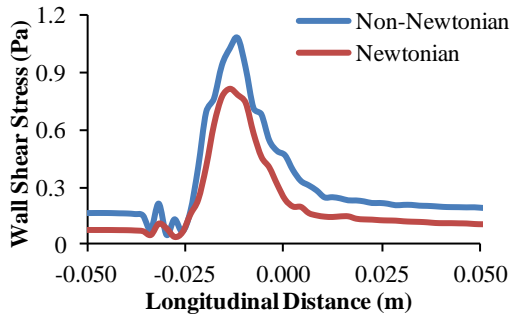Peak WSS in the fully developed flow is about 33% higher for non-Newtonian flow in

Figure 2. Vena cava wall shear stress for Newtonian and Non-Newtonian blood viscosity models. Distance is measured from the tip of the filter.

comparison to the corresponding Newtonian condition (Figure 2). Moreover, non-Newtonian fluid assumption yields almost 100% higher resting WSS as opposed to Newtonian fluid. Thus the non-Newtonian blood viscosity model is a valid assumption for determining the characteristics of the filter.
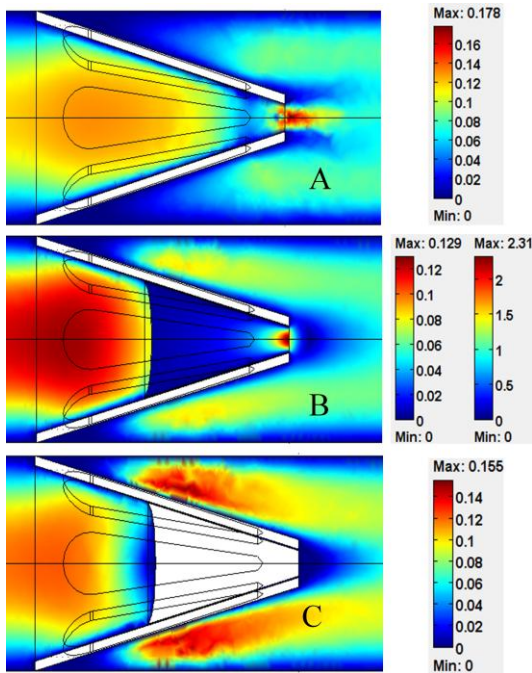

Figure 3. Velocity profiles along axial centerline for initial state where no clot is modeled (A), an intermediate state with porosity $(\varepsilon_C = 0.5)$ and permeability $(\kappa_C = 5 \times 10^{-7} \text{ m}^2)$ (B), and final state where clot modeled with no-slip conditions (C). Blood flow direction is from left to right. Left and right color bar represent blood velocity in the vena cava and clot, respectively.

3.2: Effect of clot accumulation

The composition of blood clot changes over time. In the early stage, the clot has porous structure though which blood can flow but as time progresses, the clot becomes too rigid to allow any blood flow through it. Therefore, progression of clot accumulation in the filter was modeled by changing the porosity and permeability of the clot structure. Initial stage was assumed as the absence of any clot whereas, rigid clot was assumed at the final state.

Velocity profiles at different stages of clot accumulation reveals that as clot matures, velocity increases around the tip and along the outer filter edge indicating the reduction of stagnant zones (Figure 3). On the other hand, recirculation region increases at the immediate proximal of the filter tip with clot accumulation.

Both permeabilties and porosities of clot structure decrease as clot accumulates and result reduction in blood flow through the clot. The restricted bloods try to go through the side edge and thus enhance the WSS (Figure 4 and 5). Almost two-fold peak WSS is observed at the final state of clot in comparison to the initial state. Three order-of-magnitude decrease in permeability results 72% higher WSS, whereas 75% decrease in clot porosity results 30% higher WSS.

Shear stress dramatically changes adjacent to the filter. Non-uniform shear stress patterns are observed along both the radial and longitudinal directions (Figure 6). Maximum shear stress are
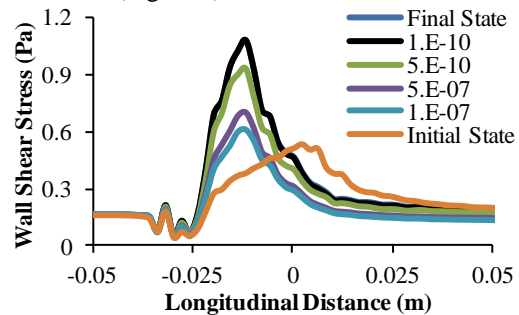

Figure 4. Wall shear stress patterns for different clot permeabilites correspond to different stage of clot accumulation. Distance is measured from the tip of the filter.
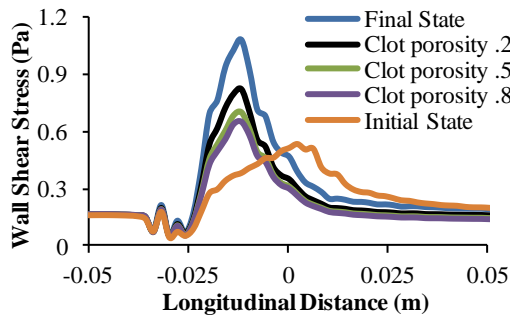
Figure 5. Wall shear stress patterns for initial state, variable porosities from 0.2 to 0.8 and final state of clot accumulation. Distance is measured from the tip of the filter.

found in the cross-section just distal to the blood clot, whereas minimal shear stress are found in the cross-sections just proximal to the exit of the filter. Heterogeneity in shear stress patterns imply that thrombogenicity varies depending on the position and state of clot accumulation.
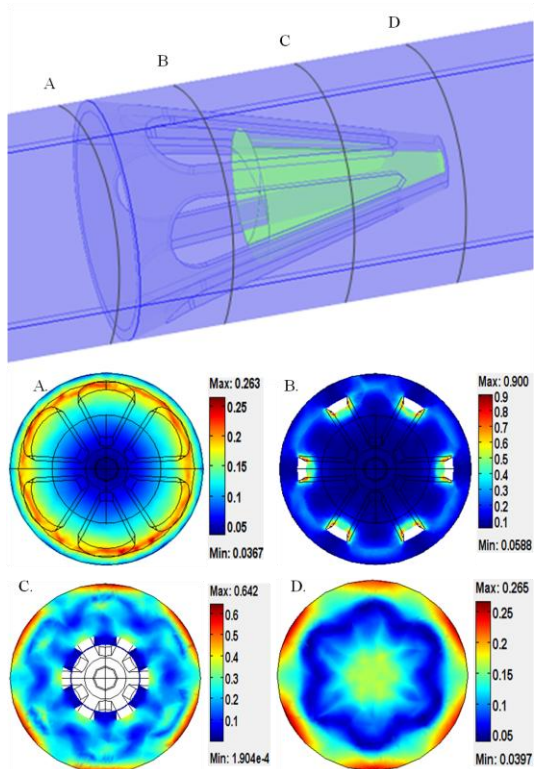

Figure 6. Shear stress at the cross-sections along the axial centerline given at values of -.034 m (A), -.025 m (B), -.01 m (C), and .0025 m (D) as measured from tip of filter. Color bars represent the shear stress.

4. Conclusions

A computational model that characterizes the local hemodynamics after a candidate filter deployment has been developed. Significant differences in shear stress patterns between non-Newtonian and Newtonian viscosity models validate the use of the Non-Newtonian model given the variability in viscosity due to shear rate of fluid flow. Reduction in porosity and permeability due to clot accumulation yield increased WSS. Non-uniform shear stress patterns along longitudinal and radial directions of IVC may indicate variability in regions along caval wall that create potential predisposition to filter induced thrombosis. This study provides important insights on future safe and effective use of IVC filter. Although CFD models could characterize the local hemodynamics after filter deployment, experimental validation is required to fully evaluate the candidate filter design.

5. References

[1] Beckman, M.G., Hooper, W.C., Critchley, S.E., Ortel, T.L., Venous thromboembolism: a public health concern, Am. J. Prev. Med., 38(4 Suppl), pp. S495-501 (2010).
[2] PREPIC Study Group, Eight-year follow-up of patients with permanent vena cava filters in the prevention of pulmonary embolism: the PREPIC (Prevention du Risque d'Embolie Pulmonaire par Interruption Cave) randomized study, Circulation, 12(3), pp. 416-422 (2005).
[3] Singer, M.A., Henshaw, W.D., Wang, S.L., Computational modeling of blood flow in the TrapEase inferior vena cava filter, J. Vasc. Interv. Radiol., 20, pp.799-805 (2009).
[4] Kroll, M.H., Hellums, J.D., McIntire, L.V., Schafer, A.I., Moake, J.L., Platelets and shear stress, Blood, 88(5), pp.1525-1541 (1996).

6. Acknowledgements